Real-time analysis of platelet aggregation and procoagulant activity during thrombus formation in vivo

Real-time analysis of platelet aggregation and procoagulant activity during thrombus formation in vivo

Tadataka Hayashi,[1,2] Hideo Mogami,[2,4] Yusuke Murakami,[2,3] Toshio Nakamura,[1] Naohiro Kanayama,[3] Hiroyuki Konno,[1] and Tetsumei Urano[2]

[1]Second Department of Surgery, [2]Department of Physiology, [3]Department of Obstetrics and Gynecology, Hamamatsu University School of Medicine, Hamamatsu, Japan. [4]Bioenvironmental Science, Okazaki Institute for Integrative Bioscience, Okazaki, Japan.

Address correspondence to Hideo Mogami, Department of Physiology, Hamamatsu University School of Medicine, Handa-yama 1-20-1, Higashi-ku, Hamamatsu, Shizuoka, 431-3192, Japan. Phone: 81-53-435-2249; Fax: 81-53-435-7020; E-mail: hmogami@hama-med.ac.jp.

Abstract

The exact mechanism of blood vessel thrombus formation remains to be defined. Here, we introduce a new approach to probe thrombus formation in blood vessels of living animals using intravital microscopy in green fluorescent protein (GFP)-transgenic mice to simultaneously monitor platelet aggregation and procoagulant activity. To this end, GFP-expressing platelets and annexin A5 labeled with a fluorescent dye were employed to visualize and analyze platelet aggregation and markers of procoagulant activity (platelet surface phosphatidylserine, PS). Laser-induced thrombi increased and then decreased in size with time in vessels of living animals, whereas platelet surface PS initiated at the site of injury and then penetrated into the thrombus. PS-positive platelets were predominantly localized in the center of the thrombus, as was fibrin generation. The experimental system proposed here is a valuable tool not only for investigating mechanisms of thrombus formation but also to assess the efficacy of anti-thrombotic drugs within the vasculature.

key words: platelet aggregation, procoagulant activity, phosphatidylserine, calcium signaling, GFP transgenic mice, intravital microscopy

Introduction

Since platelet aggregation was first measured by the turbidimetric method of Born [1], much progress in understanding platelet aggregation and the coagulation process has been made. However, we have yet to uncover the exact mechanism of thrombus formation in the blood vessel. Because platelets are easily activated ex vivo, it is difficult to extrapolate the data obtained from in vitro studies to the in vivo situation. It is now crucial to verify in vitro data in a more physiological situation to obtain a detailed understanding of the mechanism of thrombus formation.

Currently, on the basis of in vitro experiments, the basic mechanism of thrombus formation is thought to be sequential events consisting first of platelet adhesion, then aggregation and finally blood coagulation at the site of vascular injury. While platelets remain at the site of injury despite blood flow, morphological changes do take place together with a transient elevation of the intracellular calcium concentration ($[Ca^{2+}]_i$). The latter triggers additional secretion of Ca^{2+}-mobilizing agonists, such as ADP, from dense granules and causes Ca^{2+} influx, which in turn results in sustained elevation of $[Ca^{2+}]_i$ in platelets [2-5]. This induces exposure of phosphatidylserine (PS) at the platelet surface via activation of scramblase from the inner leaflet of the platelet plasma membrane to the outer leaflet, and inhibition of translocase, which exerts the opposite action on PS. PS exposure provides a catalytic surface for conversion of prothrombin into thrombin through the formation of prothrombinase complex, which is essential for the development of procoagulant activity, and finally leads to fibrin clotting [6] . However, these observations have not yet been extensively confirmed in the vessels themselves and not at all in veins. The question then arises as to how and where platelets acquire procoagulant properties by exposing PS during thrombus formation within the vasculature. The present study was conducted to establish an approach of the study of platelet aggregation and its procoagulant properties in the vessels of living animals and to verify the in vitro data in vivo.

Recent advances in genetic engineering and optical instrumentation have allowed us to investigate thrombus formation within the circulation [7-9]. In order to visualize and analyze the mechanism of thrombus formation in situ, we employed transgenic mice that express green fluorescent protein (GFP) in all tissues (except erythrocytes and fur) [10], and fluorescent dye-labeled annexin A5, a protein binding specifically to PS [11,12], as a marker of procoagulant activity [13]. In vitro experiments were first performed to examine the relationship between changes in $[Ca^{2+}]_i$ and PS exposure on the platelet surface using epifluorescence microscopy. The total amount of PS exposed on the platelet surface increased in a Ca^{2+}-dependent manner. Second, we conducted an in vivo study of laser-induced thrombi in the blood vessels of GFP mice using intravital confocal microscopy. Thrombi initially increased and then decreased in size, measured as fluorescence intensity of GFP expressed in platelets, whereas PS exposure in the thrombi increased with time, measured as annexin A5. The subsequent introduction of Ca^{2+} ionophore via an intravenous route resulted in further penetration of PS exposure to the luminal surface of a thrombus.

These observations indicate that increasing amounts of PS evoked by a Ca^{2+} signal in thrombi lead to initiation of coagulation within the vasculature. Changes in fluorescence intensity of both probes in the thrombi could be modulated by pretreating the mice with either aspirin or U73343 [14], a non-specific tyrosine kinase inhibitor. Here, we have established an in vivo approach to analyze platelet aggregation capacity and procoagulant activity, and have verified the in vitro data in vivo during thrombus formation.

Materials and methods

Animals. Green fluorescent protein (GFP)-expressing transgenic C57BL/6J mice were supplied by Dr. Okabe (Osaka University, Osaka, Japan) [10]. Tie2/GFP-expressing FVB/N transgenic mice were obtained from Jackson Laboratory (Bar Harbor, ME) [7]. Wild-type (WT) C57BL/6J mice were obtained from SLC (Shizuoka, Japan). The experimental protocol was reviewed and approved by the Animal Experiments Committee of Hamamatsu University School of Medicine.

Materials. Acetylsalicylic acid (aspirin) was obtained from Wako (Osaka, Japan). U73343 was from Alexis Biochemicals (Lausen, Switzerland). Alexa Fluor 568, 488 and fluo-4 AM were from Molecular Probes (Eugene, OR). Annexin A5 was donated by KOWA Pharmaceuticals (Tokyo, Japan) and mouse antibody against the human fibrin IIβ chain (Bβ15-42) was purchased from Accurate Chemical (Westbury, NY). Ionomycin, thrombin, collagen type I and all other chemicals were purchased from Sigma (St. Louis, MO). Human fibrinogen was obtained from Enzyme Research Laboratories, Inc (South Bend, IN). Multiple calcium-binding site mutant of annexin A5: Four calcium-binding site mutant of annexin A5 was produced by digesting and ligating cDNA of each single mutant into the other [15].

Solutions. The Hepes buffer solution for platelet preparation contained 137 mM NaCl, 2 mM KCl, 12 mM $NaHCO_3$, 0.3 mM NaH_2PO_4, 1 mM $MgCl_2$, 5.5 mM glucose, 0.02 U/ml apyrase and 5 mM Hepes-NaOH (pH 7.3). The standard extracellular solution contained 140 mM NaCl, 5 mM KCl, 1 mM $MgCl_2$, 2.5 mM $CaCl_2$, 10 mM glucose, 1 mM pyruvate and 10 mM Hepes-NaOH (pH 7.3). In some experiments, $CaCl_2$ was not included in the extracellular solution.

Platelet preparation. Mice were anesthetized with intraperitoneal sodium 5-ethyl-5-(1-methylbutyl) barbiturate (Nembutal; 50 mg/kg, Dainippon Sumitomo Pharma, Japan) in an atmosphere of diethyl ether. Blood samples were collected from the inferior vena cava with a syringe containing 0.1 volumes of 3.8% trisodium citrate. Platelet-rich plasma (PRP) was prepared by centrifugation at 100 g for 10 min at 22°C. After removal of the PRP, platelet-poor plasma (PPP) was obtained from the supernatant by centrifugation at 1,800 g for 10 min. We adjusted the concentration to $3x10^5$ platelets/μl PRP with autologous PPP using a whole-blood cell counter (Celltac, Nihon Kohden, Tokyo, Japan). Washed platelets from the PRP were prepared by further centrifugation at 700 g for 10 min and resuspended in the HEPES buffer.

Measurement of aggregation. Platelet aggregation was measured in PRP stirred at 1,000 rpm by the

turbidimetric method of Born [1] using a lumi-aggregometer (PAT-2M, SSR Engineering Co., Ltd., Tokyo, Japan). The aggregometer was calibrated with PRP for zero light transmission and with PPP for 100% transmission. Changes in light transmission were recorded for 10 min. Collagen-induced aggregation in PRP was measured with addition of 0.1 volumes of collagen. Aspirin was dissolved in 0.1 M sodium bicarbonate ($NaHCO_3$) and its pH was adjusted to7.4 with NaOH.

In vitro imaging experiments. Fluorescence images were captured using an Olympus inverted microscope (60x NA 1.45, oil immersion objective) equipped with a cooled (-50ºC) coupled charge device digital camera (ORCA-ER; Hamamatsu Photonics, Hamamatsu, Japan). Captured images were analyzed on an Aquacosmos imaging station (Hamamatsu Photonics). The excitation light source was 150 W xenon lamp with a Hamamatsu Photonics monochromator (C7773). Triple band pass filter (XF68-1, Omega optical, Brattleboro, VT) was used for measurement of fluo-4 or GFP and Alexa Fluor 568.

Dual monitoring of intracellular Ca^{2+} concentration ($[Ca^{2+}]_i$) or GFP-expressing platelets and surface-exposed PS. Washed platelets from either WT or GFP mouse PRP were prepared as described above. For simultaneous measurement of $[Ca^{2+}]_i$ and PS exposure, the washed platelets from WT mice were loaded with 5 μM fluo-4 in Hepes buffer for 45 min at room temperature. Annexin A5 labeled with Alexa Fluor 568 (ANX) was used as a marker of surface-exposed PS on the platelets [13,16]. The fluo-4-loaded platelets were allowed to adhere to glass bottomed dishes coated with 1 mg/ml-fibrinogen for 15-20 min and were then perfused continuously with the extracellular solution from a gravity-fed system at room temperature, unless otherwise noted. The light emission of fluo-4 or GFP excited by 488 nm and ANX excited by 568 nm was collected through a triple band pass filter. Their fluorescence intensity was normalized to each initial value; the relative fluorescence change is referred to as the "relative intensity."

In vivo Imaging experiments

Intravital fluorescence confocal microscopy. For intravital fluorescence microscopy of the microcirculation of a living mouse, we used a Yokogawa Real Time 3D Workstation, composed of a Nikon TE 600 microscope (40x, NA 0.8 or 60x NA 1.0 water immersion objective), a Yokogawa CSU-21 confocal scanner unit, either EB-CCD or EM-CCD (C7190 or C9100-12, Hamamatsu Photonics) and a piezo electric driver (P-721.17, Physik Instrumente GmbH & Co. KG, Germany), with which a focal plane image (one optical section) can be taken at 33 ms along the z axis. GFP and Alexa Fluor 568 were simultaneously excited by 488 and 568 nm lasers (Krypton Argon-ion lasers; 643-YB-A01, Melles Griot Laser Group, CA). For the simultaneous monitoring of both fluorescent wavelengths, an emission beam splitter, a W-view Optics (A 4313-11, Hamamatsu Photonics), was installed between the scanner unit and the CCD. The W-view consists of a dichroic mirror of 550 nm, two emission filters, 510/23 nm band pass filter for GFP and 590 nm long pass filter for Alexa Fluor 568 excited by 568 nm, so that two separate images of GFP and Alexa Fluor 568 fluorescence can be produced at the same time.

Laser-induced vessel-wall injury. Mesenteric venules were identified and endothelial injury was induced

by a 514 nm argon ion laser, (543-GS-A03; Melles Griot Laser Group, CA). The laser beam was aimed at the endothelium through the microscope objective lens. The laser-injured area of endothelium, the diameter of which was approximately 10 μm, was kept constant by changing intensity and duration of laser illumination.

GFP mouse preparation for in vivo imaging. GFP mice were anesthetized with intraperitoneal Nembutal (50 mg/kg, Dainippon Pharma) in an atmosphere of diethylether. A cannula was placed into the tail vein of each animal for injection. Mice were placed in a supine position on the stage of the intravital fluorescence microscope. A midline laparotomy incision was made, and then the mesentery of the ileum was pulled out of the abdomen and draped over a plastic mound. The mesentery was continuously perfused with 37°C-warmed saline to prevent the vessels from drying out. For visualizing the surface-exposed PS in a thrombus, ANX (2 μg/g mouse body weight) was administered into the tail vein 15 min before laser injury. To detect fibrin generation in a thrombus, Alexa Fluor 568-labeled anti-human fibrin IIβ chain (2 μg/g mouse body weight) was injected into the tail vein of the WT mice 30 min before laser injury. Changes in fluorescence intensity were measured with the combination of EB-CCD and an image intensifier (C8600-04, Hamamatsu Photonics).

Image Analysis. A z-stack of 40 optical sections at up to 30 frames per second from the vessel wall to the luminal surface of a thrombus were captured every 5 s (1-μm optical slice thickness, 40 z-sections collected at 1-μm intervals) and analyzed using a Yokogawa Real Time 3D Workstation and IPLab software (BD Biosciences Bioimaging, MD). A freehand-defined region of interest (ROI) was traced along the outline of fluorescent areas. The fluorescence intensity of GFP was normalized to the initial value in each experiment, whereas that of ANX was normalized to the last value. To obtain the perpendicular plane of merged images of PS-positive and -negative platelets, sequential focal plane images (optical sections) of GFP and ANX fluorescence were merged and reconstructed into 3D images of a thrombus using VoxBlast 3.1 (VeyTek Inc. Fairfield, AI).

Statistics. Data are given as means ± S.E. Statistical significance was evaluated using Student's *t* test.

Results

Validation of the ability of GFP-expressing platelets to aggregate in response to collagen using a turbidimetric aggregometer. We first tested the ability of GFP-expressing platelets to aggregate in response to collagen, and then the effect of aspirin and U73343, a non-specific tyrosine kinase inhibitor [14], on such collagen-evoked aggregation. PRP from GFP mice stimulated with either 5 or 10 μg/ml collagen showed typical irreversible aggregation, which was comparable to that of WT mouse platelets from three independent experiments. No significant difference between them was detected at this concentration. Collagen-evoked aggregation of platelets was markedly inhibited using PRP pretreated with either 0.5 mg/ml aspirin or 20 μM U73343 (Fig. 1).

Sustained $[Ca^{2+}]_i$ elevation but not Ca^{2+} oscillations induce surface-exposed PS. It is well known that there is a close relationship between the Ca^{2+} signal as a second messenger and platelet procoagulant activity [16,17]. Therefore, we next sought any association between changes in $[Ca^{2+}]_i$ and the amount of surface-exposed PS in single washed platelets of WT mice. Because annexin A5 is a placental-derived protein with a high affinity and a strict specificity for PS in the presence of physiological concentrations of calcium ion (~2mM), it is a very useful probe to examine platelet procoagulant activity [13,18-20]. We employed Alexa Fluor 568 labeled-annexin A5 (ANX) to visualize PS exposure on the outer leaflet of the platelet plasma membrane. We simultaneously monitored changes in relative fluorescence intensity of fluo-4 and ANX in fluo-4-loaded platelets on a fibrinogen-coated glass bottomed dish. Platelets adhering to the fibrinogen showed spontaneous Ca^{2+} oscillations without any change in fluorescence intensity of ANX, indicating absence of surface-exposed PS (Fig. 2A) (N=30 cells from 3 independent experiments). In contrast, sustained $[Ca^{2+}]_i$ elevation induced by ionomycin (IMC), a Ca^{2+} ionophore, immediately increased the relative fluorescence intensity of ANX, indicating that PS became exposed on the platelet surface following sustained $[Ca^{2+}]_i$ elevation (Fig. 2B) (N=41 cells from 3 independent experiments). A similar result was obtained with thrombin stimulation (data not shown). Next, experiments were performed to confirm the applicability of the probe in the fluo-4 loaded platelets of WT mice and the GFP-expressing platelets. ANX was displaced from the platelet surface by reducing the extracellular Ca^{2+} concentration from 2.5 mM to 0.25 mM (data not shown), suggesting that the accumulation of ANX is dependent on the ambient Ca^{2+}concentration. In addition, no change in fluorescence intensity of ANX of the multiple Ca^{2+}-binding site deletion mutant [15] was detected on application of IMC. Notably, sudden loss of the fluo-4 dye occurred concurrently with morphological changes of the platelets following sustained $[Ca^{2+}]_i$ elevation indicating a change of membrane permeability (Fig. 2B and 2C, Supplementary Fig. 1; movie 1). GFP-expressing platelets stimulated with IMC behaved in the same way (Fig. 6A).

Total amount of surface-exposed PS is dependent on $[Ca^{2+}]_i$. Next, we evaluated the total amount of surface-exposed PS induced by IMC in single platelets because platelet procoagulant activity is determined by the extent of PS exposure on the surface upon both Ca^{2+}-dependent activation of scramblase and Ca^{2+}-dependent inhibition of translocase [6,21]. First, we confirmed an IMC dose-dependent elevation of $[Ca^{2+}]_i$ (Fig. 3A). Second, the latent period up to the initial binding of ANX and its total binding after stimulation by IMC at 10 μM was compared with those at 100 nM in single GFP-expressing platelets. Calibration was carried out to achieve standardization of the total amount of IMC-evoked PS exposure in this series of experiments. The extracellular solutions containing the several known concentrations of ANX were introduced at the end of each experiment, following IMC stimulation. Fig. 3B shows a representative experiment where application of 10 μM IMC resulted in more rapid binding of ANX and greater total binding than that of 100 nM IMC. Fig. 3C shows that the average increase in the concentration of ANX at 10 μM is significantly greater than at 100 nM inonomycin. The

percentage of ANX-labeled platelets was plotted as a function of time at intervals of 1 min. Almost all the platelets were labeled by ANX within 1 min following application of 10 μM whereas a bell-shaped distribution of ANX-labeled platelets with a peak at 3 min was seen with 100 nM IMC (Fig. 3D). Fig. 3E shows a representative image of ANX-labeled platelets after exposure to 100 nM IMC. Similar results were obtained in single WT platelets (data not shown). Together, these observations indicate that the higher and more prolonged $[Ca^{2+}]_i$ elevation of the platelets, the more PS is exposed on the platelet surface. On the basis of in vitro data described above, it would be sufficient to reassure that GFP platelets are phenotypically identical to WT platelets regarding platelet aggregation and Ca^{2+}-dependent PS exposure.

A growing thrombus induced by laser irradiation and laser injury site of endothelium. Based on the above in vitro data, we performed in vivo experiments using GFP mice. A very limited area of endothelium in the mesenteric venules of the GFP mice was superficially injured by laser to initiate thrombus formation without recourse to surgical intervention [8,9]. A laser-induced thrombus, approximately 10 μm in diameter (Fig. 4Aa), was consistently made by changing the intensity (90-100 mW) and duration (3-5 seconds) of laser irradiation. A circular formation of smooth muscle cells seen under the thrombus was not disturbed (Fig. 4A), indicating superficial laser injury of the venules. Furthermore, in order to measure the actual size of the injury site and to examine the extent of laser injury, transgenic mice with vascular endothelial cells (VECs) expressing GFP [7] were employed. A representative image in Fig. 4B shows the 10 μm punch-out region of the VEC caused by the laser. This region is most likely responsible for a laser-induced thrombus.

PS exposure on the platelet surface initiates at a laser-injured endothelial site and spatially develops with time during thrombus formation. The size of a laser-induced thrombus and PS exposure on the platelet surface was evaluated by measuring changes in relative fluorescence intensity of GFP and ANX (Supplementary Fig. 2; movie 2) in the same confocal plane. The spatial distribution of platelets with exposed PS in a thrombus was probed with the help of a piezo-electric driver which allows us to take focal plane images at up to 30 frames per second along the z axis (Supplementary Fig. 3). The saline containing ANX (2 μg/g mouse body weight) was administered to the GFP mice via the tail vein before laser injury, and changes in fluorescence intensity of GFP and ANX were simultaneously monitored with a beam splitter. Fig. 5A and 5B show that a laser-induced thrombus initially increased and then decreased in size whereas the area of surface-exposed PS in the thrombus increased with time. The ANX signal was almost undetectable at the site of laser injury, where blood flow sometimes detached a thrombus containing platelets exposing PS. This indicates an absence of PS-positive VECs at the site of injury (data not shown). Therefore, PS exposure on the platelet surface initiated at the site of injury (Fig. 5Aa and 5Ba) and propagated into the thrombus. As shown in Fig. 5C, this observation was verified as a relative change in the fluorescence intensity of GFP and ANX. The former increased and reached a peak at around 70 s, and then decreased, whereas the latter gradually increased with time. No change in fluorescence

intensity of ANX of the Ca^{2+}-binding site deletion mutant was detected under the same experimental conditions.

Localization of PS-positive platelets in the thrombus. Next, we investigated the spatial distribution of PS-positive platelets in stabilized thrombi 5 min after laser injury. Fig. 5D shows a representative experiment of this type (N=10 thrombi from 10 mice). As shown in Fig. 5C, the relative fluorescence intensity of ANX in the thrombus reached a plateau at 5 min such that the fluorescence intensity of GFP markedly decreased at the center of the thrombus where PS-exposing platelets were predominantly localized (Fig.5D). This is probably due to loss of GFP from platelets caused by changes in their membrane permeability, because they lost fluo-4 dye under prolonged $[Ca^{2+}]_i$ elevation in vitro (Fig. 2B and 2C). The PS-positive platelets (activated platelets) were surrounded by the GFP-expressing, 'yet-to be-activated' ones. Taken together, these results indicate that surface-exposed PS spatially increases inside a thrombus, and that the initial decrease in the fluorescence intensity of GFP may be mainly due to changes in thrombus size due to blood flow, whereas the late decrease is mainly due to loss of GFP caused by changes in membrane permeability resulting from platelet activation.

Ca^{2+}mobilizing agonists evoked PS exposure on GFP-labeled platelets concomitantly with their morphological changes in a laser-induced thrombus in vivo. GFP-labeled platelets exposed PS in response to stimuli in both in vitro and in vivo experiments. These observations prompted us to probe the underlying mechanism of procoagulant activity in a thrombus by comparing PS exposure of platelets having morphological changes evoked by the Ca^{2+} mobilizing agonists, IMC and thrombin (data not shown) in vitro, with those having changes induced by laser injury and subsequent IMC application in vivo. Fig. 6A and 6B show representative images of PS-exposing platelets, which had a rounded shape with reduced GFP content under both conditions. Fig. 6Bb clearly shows PS-positive rounded platelets in a laser-induced thrombus. In contrast, the platelets that surrounded these PS-positive platelets were much brighter than those in the core of the thrombus, and they were either spheroid or discoid in shape (Fig. 6Ba). Furthermore, the sequential application of IMC (2 μg/g mouse body weight, with an expected blood concentration of at least 10 μM) via the tail vein into the stabilized thrombus 5min after laser irradiation resulted in further expansion of PS-positive rounded platelets over the entire thrombus, reaching the luminal surface of the thrombus (Fig.6C and 6D). The experimental design was rather demanding so that systemic damage to the mice was inevitable. However, as far as blood flow around a thrombus was concerned, no marked change in flow rate took place before and after administration of IMC, over a period >30 min. Importantly, peripheral PS-negative platelets had turned positive, and PS-positive platelets that had lost GFP were detected in the core of the thrombus, whereas those under blood flow hardly adhered to the thrombus. These results may indicate that the morphological similarity in adherent PS-exposing platelets under both in vitro and in vivo conditions probably results from a sustained $[Ca^{2+}]_i$.

Spatiotemporal development of fibrin generation and co-localization of PS expression and fibrin. Because Annexin A5 covers the catalytic surface provided by PS for formation of prothrombinase

complex [11,19], it is not known whether fibrin is generated in a laser-induced thrombus. We visualized the spatiotemporal development of fibrin in the thrombus by administration of Alexa Fluor 568-labeled anti-fibrin (alexa-fibrin) antibody via an intravenous route. Images were captured every 5 seconds for the first 5 min and then every 5 min afterwards and changes in the relative fluorescence intensity of alexa-fibrin antibody were monitored. Relative fluorescence intensity of alexa-fibrin antibody initially increased around the site of injury and spatially developed with time, reaching a plateau 20 min after laser injury (Fig. 7A upper panel and 7B). Heterogeneous distribution of alexa-fibrin antibody was mostly seen at the core of the thrombus, but neither at the bottom of the thrombus near the vessel wall nor at the luminal surface (Fig. 7A lower panel). This observation suggests that fibrin generation predominantly increases at the core of the thrombus as does surface-exposed PS. To examine co-localization of PS expression and fibrin formation, we introduced Alexa 488-labeled annexin A5 (ANX 488) (0.1 μg/g mouse body weight) via the tail vein at the end of the alexa-fibrin antibody experiments. This was because annexin A5 has an inhibitory effect on fibrin generation through activation of the coagulation pathway as described above. Fig. 7C shows a representative experiment of this type (N= 6 thrombi from 3 mice). Alexa-fibrin antibody was observed in the ANX 488-positive region, suggesting that fibrin is generated from PS-positive platelets in a laser-induced thrombus.

In vivo evaluation of efficacy of drugs which modify platelet aggregation and procoagulant activity. Finally, we tested using this experimental system whether the ability of platelets to aggregate and their procoagulant activity can be simultaneously evaluated. Platelets were pretreated with either aspirin (50 μg/g mouse body weight) or U73343 (1 μg/g mouse body weight), a non-specific tyrosine kinase inhibitor, by injecting them together with ANX into the tail vein of GFP mice 15 min before laser injury. Fig. 8A shows that the initial rate of increase and the peak intensity of GFP in the control and U73343-pretreated animals were essentially identical, and no increase in the intensity of GFP was seen after aspirin-pretreatment. Decreases could be seen with aspirin-treated and U73343-treated, as well as control thrombi thereafter. On the other hand, the average increase in relative fluorescence intensity of ANX after aspirin- or U74443-pretreatment was suppressed by 60% and 75%, respectively, 5 min after laser injury (Fig. 8B). These observations indicate 1) that the increase in size of the thrombus is determined by the balance between the degree of platelet-platelet tethering and dissociation due to blood flow, 2) that the two components of tethering and dissociation can be affected by aspirin and U73343 through distinct mechanisms and 3) that the inhibitory effect of aspirin on platelet-platelet tethering might affect PS exposure on the platelet surface. Thus, the effect of reagents on platelet aggregation and procoagulant activity can be simultaneously evaluated using this experimental system.

Discussion

The present study provides two lines of evidence pertinent to thrombus formation. First, we have demonstrated how and where platelets acquire procoagulant properties by exposing PS during thrombus formation within the mesenteric venules. Second, we have introduced a new approach to simultaneously monitor platelet aggregation and procoagulant activity for evaluation of the efficacy of antithrombotic drugs in living animals.

Surface-exposed PS has been employed as a marker of procoagulant activity since Wolfs et al. reported that the number of surface PS-positive platelets, assessed as fluorescent-labeled annexin A5-positive cells, is proportional to procoagulant activity measured as prothrombinase activity [21]. On the basis of this finding, we have provided further evidence from in vitro cell-based experiments that the total amount of surface-exposed PS in single platelets is dependent on $[Ca^{2+}]_i$, which cause changes in morphology and membrane permeability (Fig. 2 and 3). This is consistent with the report from Heemskerk et al [16]. The changes in morphology and membrane permeability induced by sustained $[Ca^{2+}]_i$ elevation are probably due to activation of Ca^{2+}-dependent proteases, such as calpain [20], and are similar changes taking place during apoptosis [6,22]. This evidence has here been extended into the following in vivo situation. As shown in Fig. 5 and 6, PS-exposing platelets originate at the bottom of the thrombus near the vessel wall of the mesenteric venule, where the endothelium is injured by laser irradiation, and increase in both numbers and area towards the luminal surface of the thrombus. Most PS-exposing platelets are in the core of the thrombus—but they are not at the bottom where the expression of tissue factor (TF) may initiate [23] —and are surrounded by PS-negative, spheroid- or discoid-shaped platelets labeled with GFP. In contrast, PS-positive platelets, which have lost GFP, become rounded, as seen in Fig. 6B, and further development of PS exposure into the peripheral PS-negative platelets occurred with stimulation by Ca^{2+} ionophore (Fig. 6C). The observations in Fig. 6B can be reconciled with the data in Fig. 7A showing that fibrin generation predominantly increases at the core of a thrombus, being distant from the initial PS-exposing platelets. Moreover, simultaneous acquisition of PS expression and fibrin formation showed their co-localization (Fig. 7C). Taken together, these results suggest: 1) that sustained $[Ca^{2+}]_i$ elevation induces surface-exposed PS in single platelets during thrombus formation, whereas PS is not exposed at the surface of the GFP-expressing platelets where sustained $[Ca^{2+}]_i$ elevation has yet to occur; 2) that Ca^{2+} signal-based PS exposure propagates from the vessel wall to the center of the thrombus; and 3) that fibrin generated from PS-positive platelets is mostly localized in the core of the thrombus. Platelets with a transient $[Ca^{2+}]_i$ elevation in the core of the thrombus are protected against the rheological resistance force of blood flow. These platelets would be expected to favor binding of fibrinogen through αIIbβ3 and to be exposed to a relatively high concentration of Ca^{2+}-mobilizing agonists, such as ADP, from dense granules [3,4,24,25]. Such platelet-platelet interaction may lead to prolonged $[Ca^{2+}]_i$ elevation and propagation of Ca^{2+} signals into the thrombus, thereby generating the predominant area of PS exposure and subsequent fibrin generation in the core of the thrombus. The model proposed above can be supported by the observations that

peripheral PS-negative platelets had turned into positive ones, and that PS-positive platelets that had lost GFP were detected in the core of the thrombus whereas those under blood flow hardly adhered to the thrombus (Fig. 6C). Our data in Fig. 5C show that the peak size of the thrombus was reached about 70 seconds after laser injury. These in vivo experiments were performed on mouse mesenteric venules of ~ 200 μm diameter, where the shear rate is approximately ~100 s^{-1} [26] whereas it is 1500s^{-1} in mouse arterioles. Despite the difference between shear rates in the venules and arterioles, our observations are in good agreement with recent reports from Furie´s group of laser-induced thrombi in arterioles within the mouse cremaster muscle [27,28]. These investigators have demonstrated 1) that the average time to peak size of the thrombus is about 100 seconds after laser injury; 2) that $[Ca^{2+}]_i$ elevation occurs in the center of the thrombus but not at the periphery; and 3) that fibrin generation develops from the site of injury towards the luminal surface of the thrombus, as does TF. The simplest explanation for these similar results may be that shear rate does not affect the average time to maximum thrombus size very much once initial firm adhesion of platelets, triggered by binding of glycoprotein Ibα and von Willebrand factor, is established at the site of injury [3,26].

We have introduced a new approach for the simultaneous in vivo evaluation of platelet function and procoagulant activity by measuring relative changes in fluorescence intensity of GFP and ANX in thrombi as a function of time. The dual real-time monitoring of such parameters in comparison with the controls enables us to study specific effects of aspirin and U73343 on platelet aggregation and blood coagulation at the same time within the vasculature under normal conditions of blood flow (Fig. 8). Such information on drug-modulated thrombus formation is qualitatively distinct from data obtained from aggregometry (Fig. 1). For example, in the case of the U73343-treated mice during thrombus formation, platelet-platelet tethering was comparable to the control but earlier dissociation occurred, while platelet procoagulant activity was markedly suppressed (Fig. 8). All we could have learned from aggregometry is that collagen-evoked aggregation of platelets is markedly inhibited using PRP with pretreatment of U73343. Thus, we have also obtained dynamic information on the effect of the reagents on platelet accumulation and procoagulant activity during thrombus formation using this experimental system. The GFP-expressing platelets allow us to clearly visualize morphological changes of single platelets in a thrombus as well as changes of the entire thrombus in size. To understand the mechanisms of thrombosis such as atherothrombosis and deep vein thrombosis in the in vivo situation, new experimental models are required and can be produced by crossing GFP mice with other mouse models of vascular disease.

Conclusion

This experimental system, including the GFP mice and a fluorescent dye-labeled annexin A5, is a valuable tool not only to investigate mechanisms of thrombus formation under both physiological and pathophysiological conditions in veins and arteries but also to assess the efficacy of antithrombotic drugs

within the vasculature.

Acknowledgement

We greatly appreciate the gift of four calcium-binding site mutant of annexin A5 from Dr. Francoise Russo-Marie (Institut Cochin de Ge´ne´tiqueMole´culaire, Unite´ INSERM U332, 75014 Paris, France). We thank Dr. Satoshi Nakamura (Director for Finance and Hospital, Hamamatsu University School of Medicine) for critical discussion and Dr. Yuko Suzuki (Department of Physiology) for technical advice. This work was supported by Grant-in-Aid for Young Scientists (B: 17790885) to T.H., Grant-in-Aid for Scientific Research (C: 18590204) to T.U. from the Japan Society for the Promotion of Science (JSPS), a grant from the Smoking Research Foundation to T.U., and a grants from Takeda Science Foundation to H.M.

The abbreviations used are: PS, phosphatidylserine; ANX, annexin A5; IMC, ionomycin

References

1. Born GV (1962) Aggregation of blood platelets by adenosine diphosphate and its reversal. Nature 194:927-929
2. Rosado JA, Sage SO (2000) Phosphoinositides are required for store-mediated calcium entry in human platelets. J Biol Chem 275:9110-9113
3. Mazzucato M, Pradella P, Cozzi MR, De Marco L, Ruggeri ZM (2002) Sequential cytoplasmic calcium signals in a 2-stage platelet activation process induced by the glycoprotein Ibalpha mechanoreceptor. Blood 100:2793-2800
4. Nesbitt WS, Giuliano S, Kulkarni S, Dopheide SM, Harper IS, Jackson SP (2003) Intercellular calcium communication regulates platelet aggregation and thrombus growth. J Cell Biol 160:1151-1161
5. Jackson SP (2007) The growing complexity of platelet aggregation. Blood 109:5087-5095
6. Zwaal RF, Schroit AJ (1997) Pathophysiologic implications of membrane phospholipid asymmetry in blood cells. Blood 89:1121-1132
7. Ni H, Denis CV, Subbarao S, Degen JL, Sato TN, Hynes RO, Wagner DD (2000) Persistence of platelet thrombus formation in arterioles of mice lacking both von Willebrand factor and fibrinogen. J Clin Invest 106:385-392
8. Rosen ED, Raymond S, Zollman A, Noria F, Sandoval-Cooper M, Shulman A, Merz JL, Castellino FJ (2001) Laser-induced noninvasive vascular injury models in mice generate platelet- and coagulation-dependent thrombi. Am J Pathol 158:1613-1622

9. Falati S, Gross P, Merrill-Skoloff G, Furie BC, Furie B (2002) Real-time in vivo imaging of platelets, tissue factor and fibrin during arterial thrombus formation in the mouse. Nat Med 8:1175-1181
10. Okabe M, Ikawa M, Kominami K, Nakanishi T, Nishimune Y (1997) 'Green mice' as a source of ubiquitous green cells. FEBS Lett 407:313-319
11. Tait JF, Gibson D, Fujikawa K (1989) Phospholipid binding properties of human placental anticoagulant protein-I, a member of the lipocortin family. J Biol Chem 264:7944-7949
12. Reutelingsperger CP (2001) Annexins: key regulators of haemostasis, thrombosis, and apoptosis. Thromb Haemost 86:413-419
13. Dachary-Prigent J, Freyssinet JM, Pasquet JM, Carron JC, Nurden AT (1993) Annexin V as a probe of aminophospholipid exposure and platelet membrane vesiculation: a flow cytometry study showing a role for free sulfhydryl groups. Blood 81:2554-2565
14. Heemskerk JW, Farndale RW, Sage SO (1997) Effects of U73122 and U73343 on human platelet calcium signalling and protein tyrosine phosphorylation. Biochim Biophys Acta 1355:81-88
15. Mira JP, Dubois T, Oudinet JP, Lukowski S, Russo-Marie F, Geny B (1997) Inhibition of cytosolic phospholipase A2 by annexin V in differentiated permeabilized HL-60 cells. Evidence of crucial importance of domain I type II Ca2+-binding site in the mechanism of inhibition. J Biol Chem 272:10474-10482
16. Heemskerk JW, Vuist WM, Feijge MA, Reutelingsperger CP, Lindhout T (1997) Collagen but not fibrinogen surfaces induce bleb formation, exposure of phosphatidylserine, and procoagulant activity of adherent platelets: evidence for regulation by protein tyrosine kinase-dependent Ca^{2+} responses. Blood 90:2615-2625
17. Smeets EF, Heemskerk JW, Comfurius P, Bevers EM, Zwaal RF (1993) Thapsigargin amplifies the platelet procoagulant response caused by thrombin. Thromb Haemost 70:1024-1029
18. Thiagarajan P, Tait JF (1990) Binding of annexin V/placental anticoagulant protein I to platelets. Evidence for phosphatidylserine exposure in the procoagulant response of activated platelets. J Biol Chem 265:17420-17423
19. Thiagarajan P, Tait JF (1991) Collagen-induced exposure of anionic phospholipid in platelets and platelet-derived microparticles. J Biol Chem 266:24302-24307
20. Wolf BB, Goldstein JC, Stennicke HR, Beere H, Amarante-Mendes GP, Salvesen GS, Green DR (1999) Calpain functions in a caspase-independent manner to promote apoptosis-like events during platelet activation. Blood 94:1683-1692
21. Wolfs JL, Comfurius P, Rasmussen JT, Keuren JF, Lindhout T, Zwaal RF, Bevers EM (2005) Activated scramblase and inhibited aminophospholipid translocase cause phosphatidylserine exposure in a distinct platelet fraction. Cell Mol Life Sci 62:1514-1525
22. Orrenius S, Zhivotovsky B, Nicotera P (2003) Regulation of cell death: the calcium-apoptosis

link. Nat Rev Mol Cell Biol 4:552-565

23. Furie B, Furie BC (2005) Thrombus formation in vivo. J Clin Invest 115:3355-3362

24. Goto S, Tamura N, Ishida H, Ruggeri ZM (2006) Dependence of platelet thrombus stability on sustained glycoprotein IIb/IIIa activation through adenosine 5'-diphosphate receptor stimulation and cyclic calcium signaling. J Am Coll Cardiol 47:155-162

25. Matsui H, Sugimoto M, Mizuno T, Tsuji S, Miyata S, Matsuda M, Yoshioka A (2002) Distinct and concerted functions of von Willebrand factor and fibrinogen in mural thrombus growth under high shear flow. Blood 100:3604-3610

26. Andre P, Denis CV, Ware J, Saffaripour S, Hynes RO, Ruggeri ZM, Wagner DD (2000) Platelets adhere to and translocate on von Willebrand factor presented by endothelium in stimulated veins. Blood 96:3322-3328

27. Gross PL, Furie BC, Merrill-Skoloff G, Chou J, Furie B (2005) Leukocyte-versus microparticle-mediated tissue factor transfer during arteriolar thrombus development. J Leukoc Biol 78:1318-1326

28. Dubois C, Panicot-Dubois L, Gainor JF, Furie BC, Furie B (2007) Thrombin-initiated platelet activation in vivo is vWF independent during thrombus formation in a laser injury model. J Clin Invest 117:953-960

Figure legends

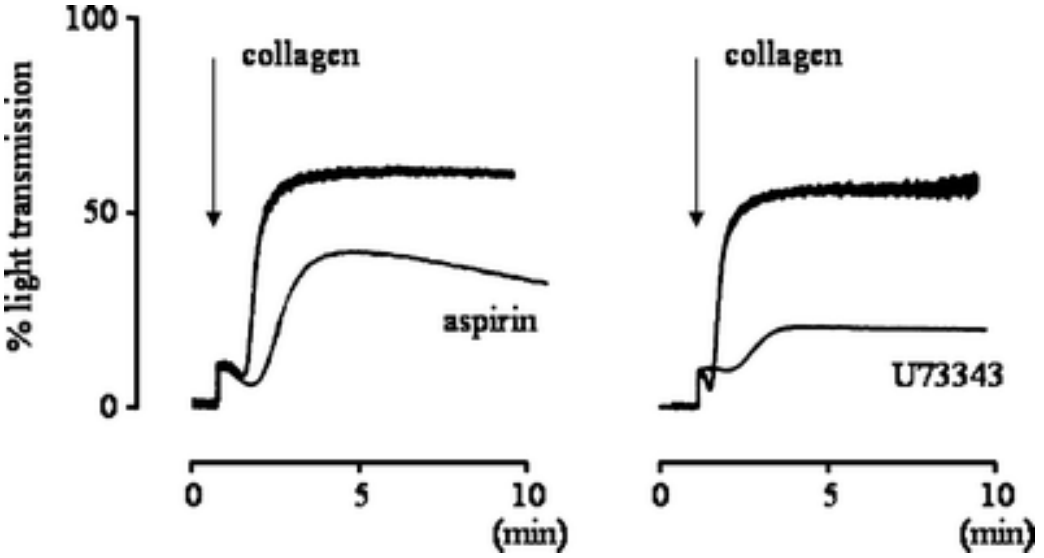

Fig. 1. *The effect of aspirin and U73343 on collagen-evoked aggregation of GFP-expressing platelets.* PRP from GFP mice was pretreated with either aspirin (0.5 mg/ml) or U73343 (20 μM) for 20 min. Collagen-evoked aggregation of the platelets was markedly inhibited by both aspirin and U73343, a non-specific tyrosine kinase inhibitor. Tracings are representative of at least 3 separate experiments

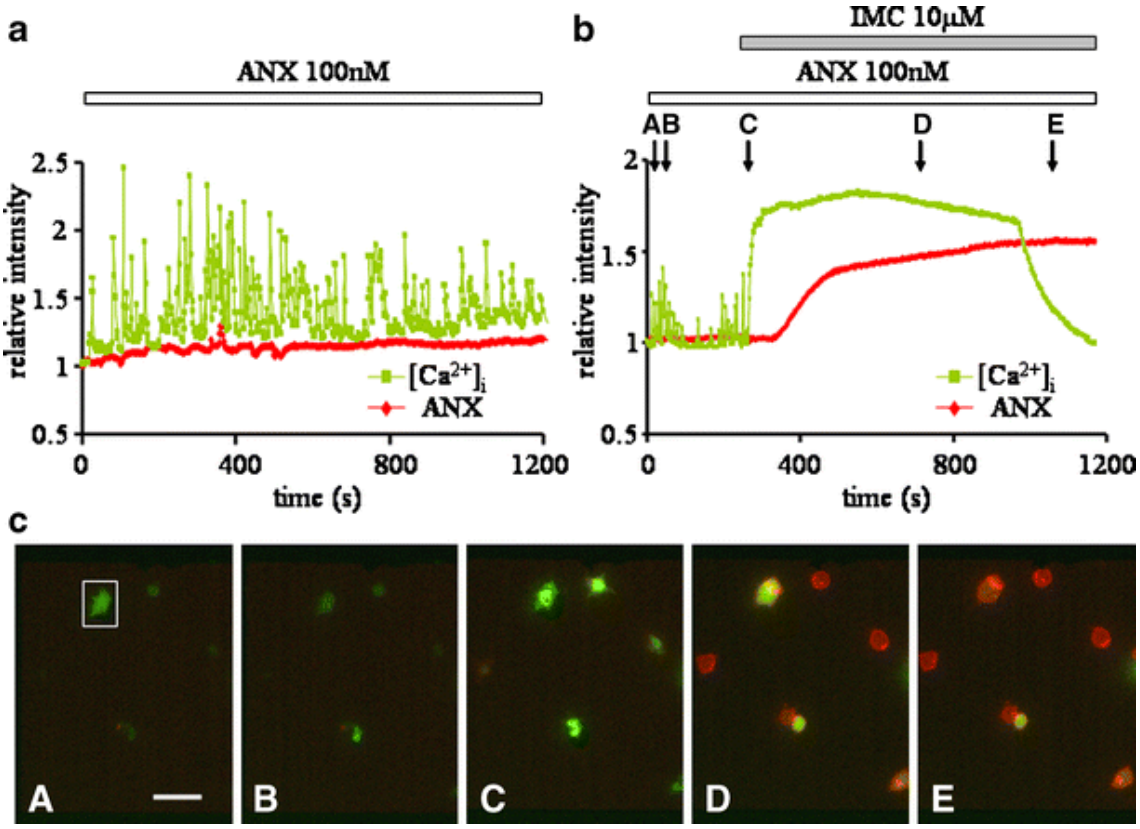

Fig. 2. *Sustained $[Ca^{2+}]_i$ elevation but not Ca^{2+} oscillations induce surface-exposed PS.* Washed platelets were prepared from WT mouse PRP and loaded with fluo-4 (green). Platelets adhering to fibrinogen (1 mg/ml)-coated glass bottomed dishes perfused with solution containing 100 nM ANX (red) are shown. (**A**) Representative trace shows that no change in the fluorescence intensity of ANX occurred in the absence of agonists while spontaneous Ca^{2+} oscillation in the fluo-4 loaded platelets lasted for more than 20 min (N=30 cells from 3 independent experiments). (**B**) Representative trace of the platelets shown in the white box in (C) (N=41 cells from 3 independent experiments). The fluorescence intensity of ANX increased following sustained $[Ca^{2+}]_i$ elevation induced by ionomycin (IMC). A sudden decrease in the fluorescence of fluo-4 was observed 800 seconds after application of IMC (**C**) The images of a-e were captured at the times indicated by the arrows in (B). Almost all the filopodia-developing platelets became rounded with increase in fluorescence intensity of ANX (red) and decrease in that of fluo-4 (green) in (e). Scale bar, 10 μm.

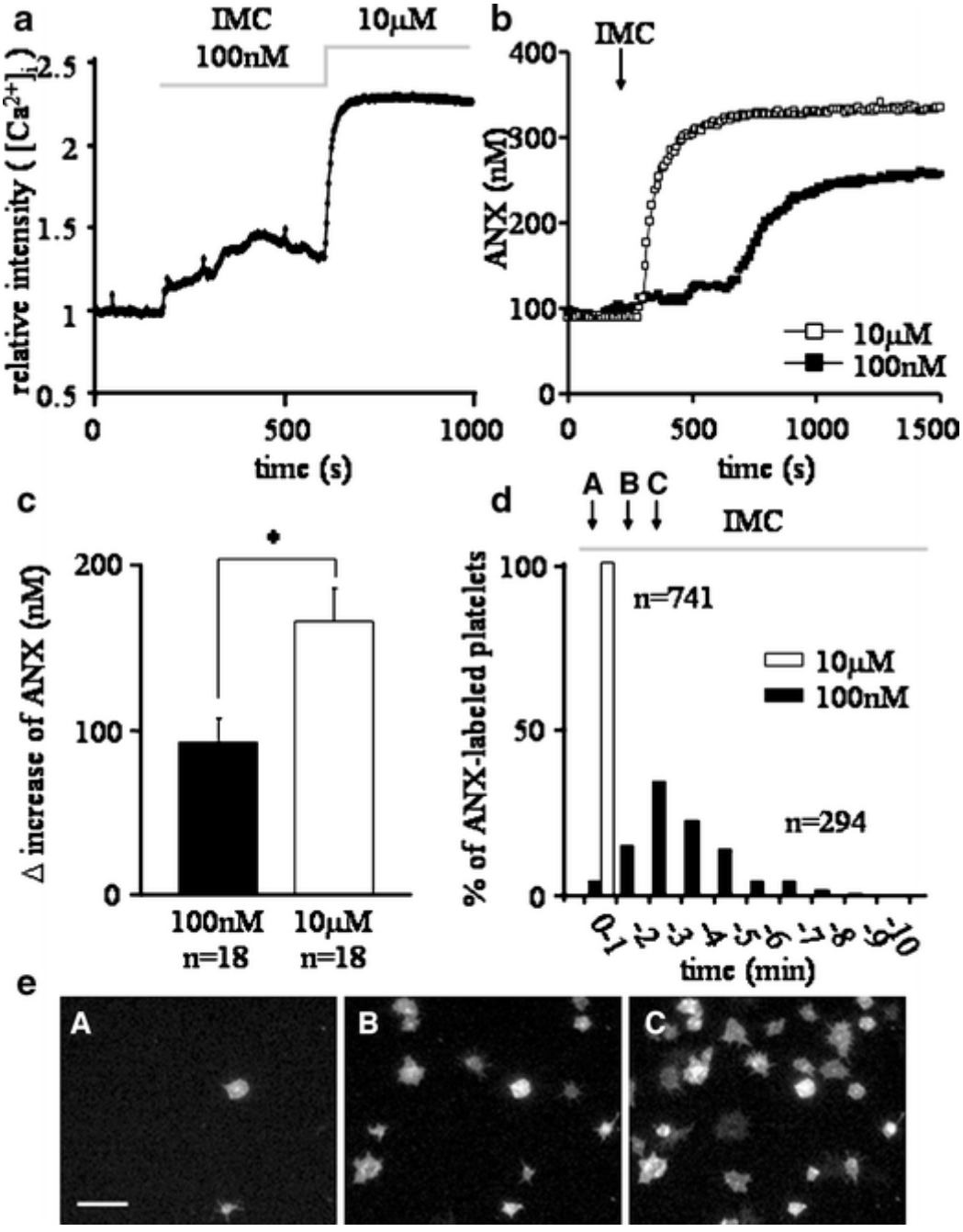

Fig. 3. *Total amount of surface-exposed PS is dependent on $[Ca^{2+}]_i$.* Washed platelets from WT mice were loaded with 5μM fluo-4 for 45 min and plated onto a fibrinogen-coated glass bottomed dish. (**A**) Washed platelets were stimulated with 100 nM and 10 μM ionomycin (IMC) sequentially. Application of IMC induced $[Ca^{2+}]_i$ elevation in a dose-dependent manner (10 μM IMC: open squares, 100 nM IMC closed squares) (N=45 cells from 3 independent experiments). (**B**) To calibrate the total amount of IMC-evoked PS exposure, the extracellular solutions containing different concentrations of ANX were introduced at the end of each experiment, following IMC stimulation. Representative trace shows that the higher the dose of IMC applied to washed platelets, the faster the binding of ANX and the greater the

increase in the total amount of ANX. (**C**) Average increase in the total amount of ANX induced by 10 μM IMC is significantly higher than by 100 nM IMC. *, $p < 0.005$. (**D**) The number of platelets labeled with ANX was counted every min and divided over the total number of ANX-labeled platelets. ANX bound to all the platelets within 1 min following stimulation with 10 μM IMC (open column) whereas the number of ANX-labeled platelets in response to 100 nM IMC (filled columns) gradually increased and reached a peak at 3 min. (**E**) The images of a-c were captured at the times indicated by the arrows in (D). ANX-labeled platelets induced by 100 nM IMC gradually increased in number and developed many filopodial projections. Scale bar, 10 μm.

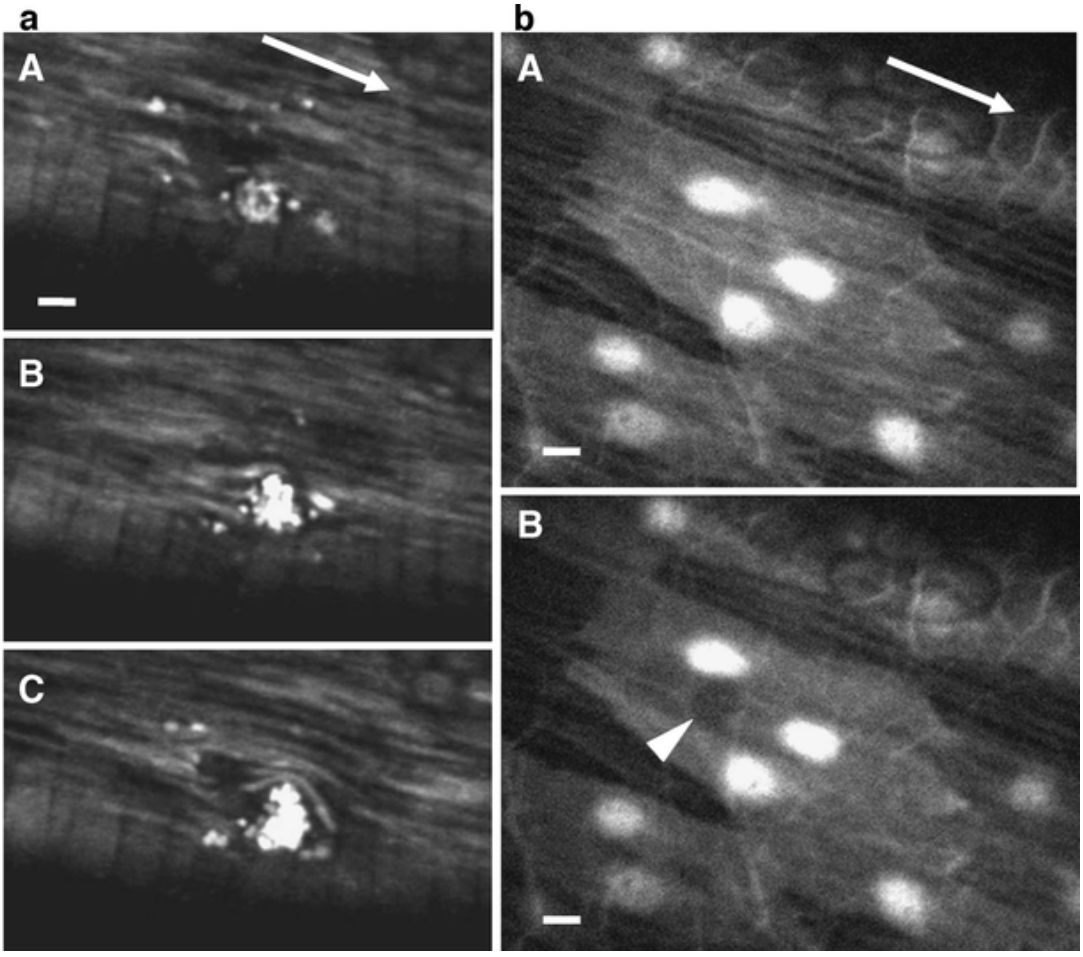

Fig. 4. *A growing thrombus induced by laser irradiation, and laser injury site of endothelium.* (**A**) The initial size of adherent platelet aggregates at the site of injury immediately after laser irradiation was ca. 10 μm (11.0±0.52 μm, N=11) in the mesenetric venules of GFP mice (a). Thereafter, the monolayer of platelet aggregates at the vessel wall grew into a rugby ball-shaped thrombus in the direction of blood flow towards the luminal side (a-c) (major axis; 37.2±1.73 μm, N=16). Note the circular formation of smooth muscle cells visible**.** (**B**) Vascular endothelial cells (VEC) were visualized in transgenic mice whose VECs express GFP. The VECs with bright GFP nuclei in parallel array formed into a line along the direction of blood flow. GFP-expressing VECs before laser injury (a). GFP-expressing VECs after laser injury (b). Laser irradiation injured a GFP-expressing VEC through an objective lens thereby inducing photobleach at the site of punch-out injury with a diameter of ca.10 μm (arrow head). Arrow shows the direction of blood flow. Scale bar, 10 μm.

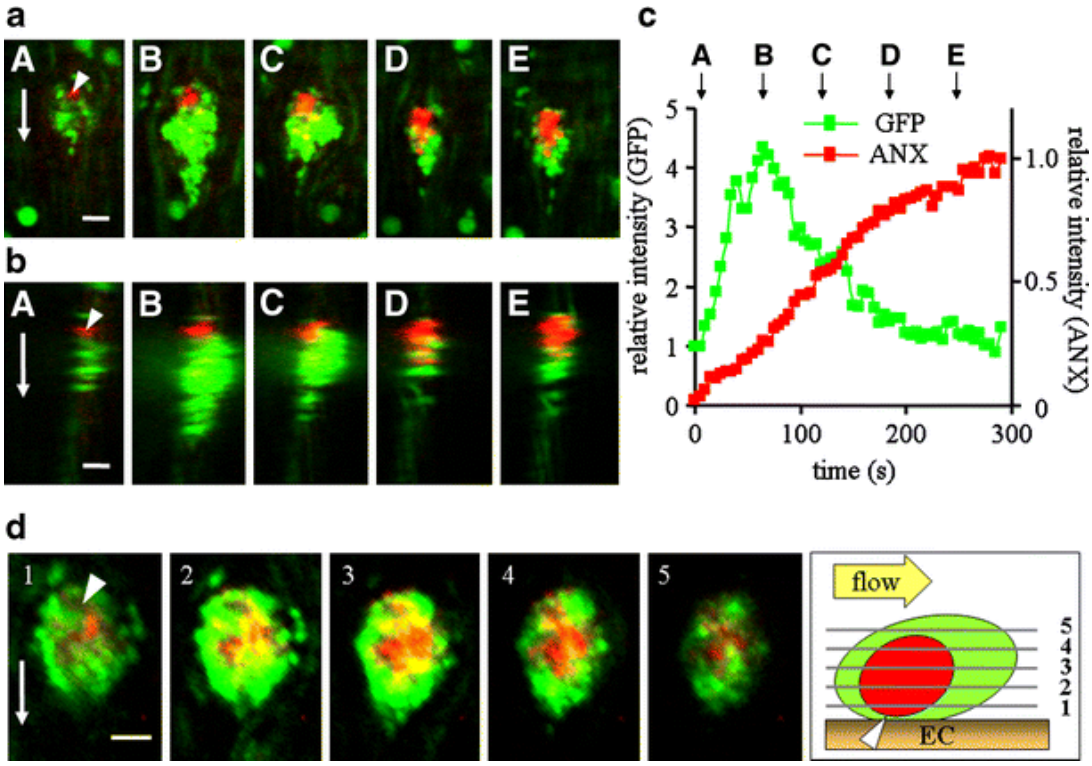

Fig. 5. *PS exposure on the platelet surface initiates at a site of laser injury and spatially develops with time during thrombus formation.* Focal plane images along the z axis from the vessel wall to the luminal surface of a thrombus were taken every 5 s for at least 5 min. Representative images and traces are shown. The images of a-e were captured at the times indicated by the arrows in (C) (N=10 thrombi from 10 mice). (**A**) Horizontal plane (X-Y) images show that a thrombus (green) increased in size at the level near the vessel wall and then decreased, whereas PS-positive platelets (red) continued to increase with time. Surface-exposed PS clearly initiated at the site of injury (arrow head) and then propagated into the thrombus. (**B**) Perpendicular plane (Y-Z) images also show that surface-exposed PS clearly initiated at the site of injury (arrow head) and developed upward towards the luminal surface of the thrombus. (**C**) Relative changes in the fluorescence intensity of GFP (green) and ANX (red) in the horizontal (X-Y) images. The peak intensity of GFP occurred around 70 s after laser injury and then decreased to baseline at 300 s whereas the intensity of ANX gradually increased and reached a plateau at 300 s, which corresponds to the changes of thrombus size and the development of surface-exposed PS (A and B), respectively. (**D**) *Localization of PS-positive platelets in a thrombus*. Five optical sections were selected at 4-μm intervals from the vessel wall to the luminal surface of a thrombus to examine the spatial distribution of PS-exposing platelets. The schematic depiction shows the perpendicular plane of a laser-induced thrombus containing PS-positive (red) and PS-negative platelets (green) on the endothelial cells (EC). The numbers in the scheme correspond to the image of each optical slice. PS-positive platelets were surrounded by PS-negative platelets in the thrombus (N=10 thrombi from 10 mice). Arrow shows the direction of blood flow. Scale bar, 10 μm

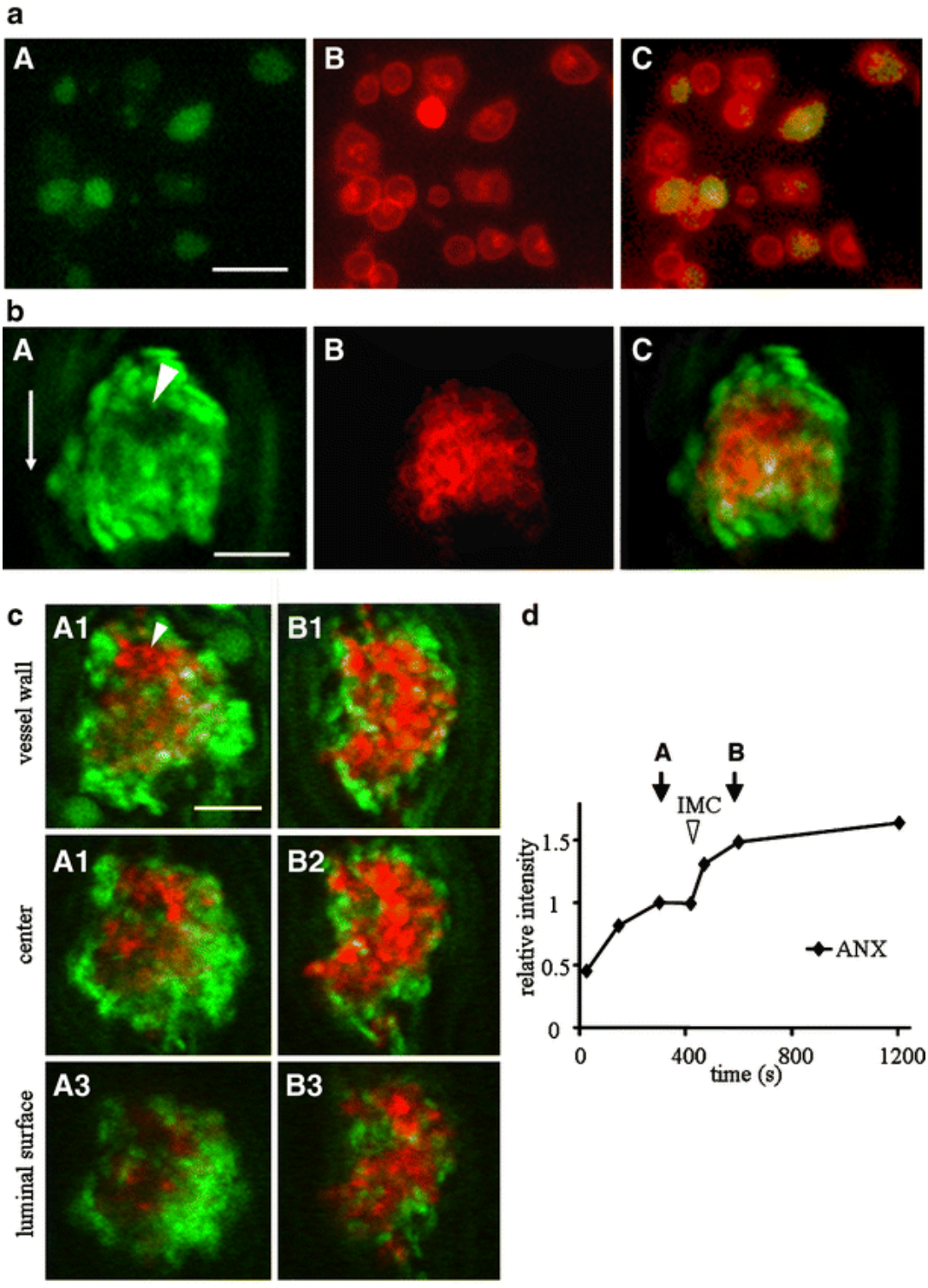

Fig. 6. *PS-exposing platelets with morphological changes under in vitro and in vivo conditions.* (**A**) Washed platelets from GFP mice were plated onto fibrinogen-coated glass-bottomed dishes. Representative images show PS-exposing platelets with morphological changes 10 min after 10 μM ionomycin (IMC) stimulation. a) Some GFP-expressing platelets were slightly fluorescent but others were

not. b) Binding of ANX to the membrane of rounded platelets with small spots of ANX inside. c) Merged images of GFP-expressing platelets and ANX. (**B**) Representative images show PS-exposing platelets with morphological changes in a stabilized thrombus 5 min after laser irradiation. a) The shapes of single GFP-expressing platelets are clearly seen in the laser-induced thrombus. In particular, those in the periphery had either discoid or spheroid shapes. Those in the center were rather dim in contrast to the peripheral platelets. b) ANX-binding platelets are rounded and their shape is very similar to those induced by IMC in vitro. c) Merged images. ANX-binding rounded platelets clustered in the center of the thrombus (N=5 thrombi from 3 mice). (**C**) The images of a and b were captured at the times indicated by the arrows in (D). Three optical sections of a thrombus (1. near vessel wall, 2. center and 3. luminal surface) were selected to compare the spatial distribution of PS-exposing platelets before (a1-a3) and after (b1-b3) IMC application. Arrow head and arrow show the site of laser injury and the direction of blood flow, respectively. Scale bar, 10 μm. (**D**) The fluorescence intensity of ANX was normalized to values at 5 min. The relative intensity of ANX was plotted as a function of time. A rapid increase in the intensity of ANX was observed immediately after application of IMC (arrow head).

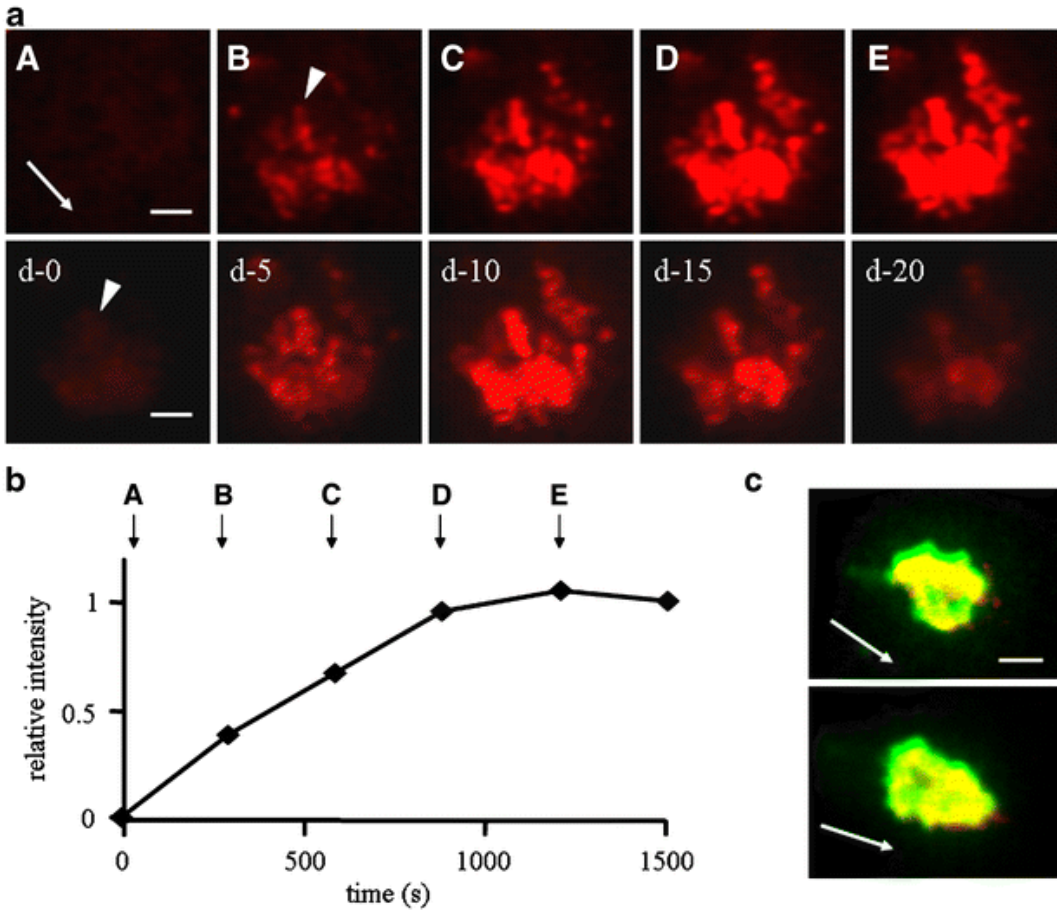

Fig. 7. *Spatiotemporal development of fibrin generation and co-localization of PS expression and fibrin.* Alexa Fluor 568-labeled anti-human fibrin IIβ chain (alexa-fibrin) (2 μg/g mouse body weight) was injected into the tail vein of WT mice 30 min before laser injury. Images were captured every 5 s for the first 5 min and then every 5 min afterwards with the combination of EB-CCD and an image intensifier, and 40x, NA 0.8 objective. Representative image and trace is shown from 5 independent experiments. Arrow head and arrow show the site of laser injury and the direction of blood flow, respectively. (**A**) The images of a-e at the level of 10-μm optical slice from the vessel wall were taken at the times indicated by the arrows in (B). The images of d0-d20 were collected every 5-μm from the z-stack of (d) optical section. Alexa-fibrin antibody started to accumulate around the site of laser injury and developed backwards into the thrombus. The fluorescence intensity of alexa-fibrin antibody reached a plateau 20 min after laser injury (e) and was maximal in the middle of the thrombus. (**B**) The fluorescence intensity of alexa-fibrin antibody was normalized to values at 20 min. Relative intensity of alexa-fibrin antibody was plotted as a function of time. (**C**) Alexa 488-labeled annexin A5 (ANX 488) (0.1 μg/g mouse body weight) was injected via the tail vein at the end of the alexa-fibrin antibody experiments (A). Two representative merged images show co-localization of alexa-fibrin antibody (red) and ANX 488 (green). Scale bar 10 μm.

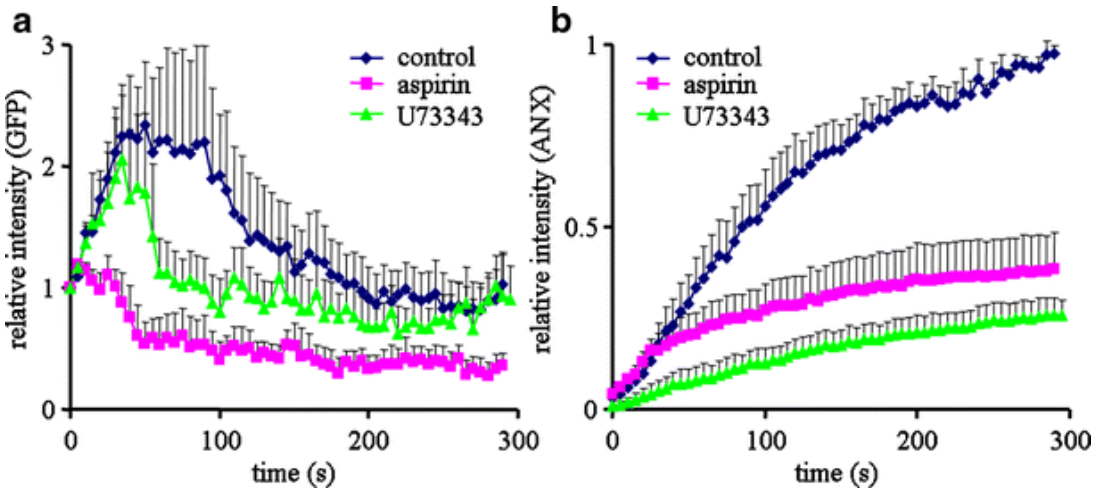

Fig. 8. *In vivo evaluation of platelet aggregation and procoagulant activity.* Platelets were pretreated with either aspirin or U73343, a non-specific tyrosine kinase inhibitor, by injecting them together with ANX into tail veins of GFP mice before laser injury. The mean values±S.E. from 5 independent experiments of 5 different venules from 3 mice are given. The fluorescence intensity of GFP and ANX was normalized to each initial value in (A) and to the last value of control experiments in (B). Average change of relative fluorescence intensity of GFP and ANX in a laser-induced thrombus plotted as a function of time. (**A**) The initial rate of increase and the peak intensity of GFP in the control (blue) and U73343-petreated experiments (green) were nearly identical, and no increase in the intensity of GFP was seen in the aspirin-pretreated case (pink). Decreases were seen with aspirin-, U73343-treated and control thrombus (**B**) The average increase in relative fluorescence intensity of ANX after aspirin- and U73343-pretreatment was suppressed by 60% and 75%, respectively, 5 min after laser injury.